Journal of Cellular Biochemistry 83:597–606 (2001)

Differences in the Uptake and Nuclear Localization of Anti-Proliferative Heparan Sulfate Between Human Lung Fibroblasts and Human Lung Carcinoma Cells

Fang Cheng,[1] Per Petersson,[2] Yolanda Arroyo-Yanguas,[1] and Gunilla Westergren-Thorsson[1]*

[1]BMC, Department of Cell- and Molecular Biology, C13, Lund University, SE-221 84 Lund, Sweden
[2]Department of Neurophysiology, Lund University, Sölvegatan 19, SE-223 62 Lund, Sweden

Abstract Heparan sulfate inhibits the proliferation of normal human lung fibroblasts (HFL-1) but not of a human lung carcinoma cell-line (A549). In this study we investigated possible mechanisms and structural requirements by which antiproliferative heparan sulfates exerts its effects on binding, uptake and subcellular localisation. Both HFL-1 and A549 cells were incubated with ^{125}I- or rhodamine-labeled L-iduronate–rich antiproliferative heparan sulfate species as well as L-iduronate-poor inactive ones. The antiproliferative heparan sulfate was bound to the cell surface on both HFL-1 and A549 cells, but to a lesser extent and with less affinity to A549 cells. Both cell types bound the antiproliferative heparan sulfate with one high- and with one low affinity site. The L-iduronate–poor heparan sulfate bound to a lesser extent and with less affinity to both cell types compared to the antiproliferative heparan sulfate. The antiproliferative heparan sulfate accumulated in the cytoplasm of HFL-1 cells after 24 h incubation, but after 72 h it was found evenly distributed in the nucleus. The time-scale for antiproliferative activity correlated with nuclear localization. In contrast, in A549 cells it was only found near the nuclear membrane. The inactive heparan sulfate was taken up in considerably smaller amounts compared to the antiproliferative heparan sulfate and could not be detected in the nucleus of either HFL-1 or A549 cells. Our data suggest that the antiproliferative activity of L-iduronate–rich heparan sulfate on normal fibroblasts may be due to direct effects on nuclear processes, such as gene transcription. J. Cell. Biochem. 83: 597–606, 2001.

Key words: heparan sulfate; antiproliferative activity; nuclear localization; confocal microscopy

The biological functions of heparan sulfate proteoglycans (HSPG) include control of cell growth and cell adhesion. This involves binding to a variety of extracellular matrix components [Elenius et al., 1990; Iozzo, 1998; Bernfield et al., 1999], such as cell adhesion molecules [Liu et al., 1998; Woods and Couchman, 1998], growth factors [Keifer et al., 1990; Gallagher and Turnbull, 1992] and cytokines [Taipala and Keski-Oja, 1997]. Binding of basic fibroblast growth factor (bFGF) to heparan sulfate (HS) is important for its interaction with the signal-transducing receptor [Keifer et al., 1990; Yayon et al., 1991]. The core proteins of HSPG are responsible for targeting the proteoglycan (PG) to their final destination whereas the HS side-chains are usually involved in the binding events. HS are highly heterogeneous glycosaminoglycans (GAGs) constructed from a repeating disaccharide (-N-acetyl-D-glucosamine (-GlcNAc)-α-1,4-D-glucuronic acid (GlcA)-β1, 4-)$_n$ backbone. This backbone can be modified in several ways. The GlcNAc residues can be deacetylated and N-sulfated (yielding Glc NSO_3) followed by epimerization at C-5 of GlcA to yield L-iduronic acid (IdoA). Subsequently

Abbreviations used: EGF, epidermal growth factor; GAG, glycosaminoglycan; GlcA, glucuronic acid; GlcNAc, N-acetylglucosamine; HS, heparan sulfate; LDH, lactate dehydrogenase; IdoA, iduronic acid; PG, proteoglycan.

Grant sponsor: Swedish Medical Research Council; Grant number: 11550; Grant sponsor: Swedish Cancer Fund; Grant sponsor: Society for Medical Research; Grant sponsor: JA Persson; Grant sponsor: G&J Kock and A Österlund Fundations; Grant sponsor: Riksföreningen mot Reumatism; Grant sponsor: Gustaf V.s 80-årsfond; Grant sponsor: A.-G. Crafoord Foundation; Grant sponsor: Thelma Zoéga Foundation; Grant sponsor: Heart Lung Foundation and the Medical Faculty, University of Lund.

*Correspondence to: Gunilla Westergren-Thorsson, BMC, Department of Cell- and Molecular Biology, C13, Lund University, SE-221 84 Lund, Sweden.
E-mail: Gunilla.Westergren-Thorsson@medkem.lu.se

Received 30 March 2001; Accepted 29 June 2001

DOI 10.1002/jcb.1254

O-sulfates can also be introduced at positions 3 and 6 of the glucosamines and at position 2 of the hexuronic acids. The final HS chain contains areas that are highly sulfated and rich in IdoA interspersed with stretches where the original backbone structure remains, and sometimes mixed regions are seen [Linker and Hovingh, 1975; Cifonelli and King, 1977; Fransson et al., 1980b; Gallagher et al., 1986; Kjellén and Lindahl, 1991; Salmivirta et al., 1996]. Heparin and HS have both stimulatory and inhibitory effects on growth depending on the type of cell. We have shown that a highly-sulfated, IdoA-rich HS fraction (HS-6) exerts antiproliferative effects on normal fibroblasts whereas a low-sulfated, GlcA-rich HS (HS-2) does not [Westergren-Thorsson et al., 1991, Arroyo-Yanguas et al., 1997]. The antiproliferative activity is dependent on chain length, the degree of sulfation and the ratio of IdoA/GlcA [Wright et al., 1989a; Westergren-Thorsson et al.,1991]. HS binds to both high affinity and to low affinity sites on the cell surface and can be internalized by endocytosis [Castellot et al., 1985; Vannucchi et al., 1988; Redini et al., 1989; Wright et al., 1989a; Arroyo-Yanguas et al., 1997]. The internalized HS can be further degraded in different cellular compartments and processed HS fragments can be transported to the nucleus in hepatocytes [Fedarko and Conrad, 1986], where they have been postulated to regulate nuclear processes [Fedarko and Conrad, 1986; Busch et al., 1992]. However, these data were based on cell fractionation, and did not provide direct identification of the cellular location of the HS. The degraded fragments could also affect various signal transduction pathways in the cell. One of the best documented effects is the inhibition of MAP-kinase activity [Ottlinger et al., 1993; Ueda et al., 1996], possibly due to a decrease in the signaling of protein kinase C [Wright et al., 1989b; Pukac et al., 1990; Herbert et al., 1996]. HS can also up-regulate the activity of various growth factors/growth factor receptors [Malmström and Westergren-Thorsson, 1998]. In order to differentiate between the binding to the cell surface receptors, uptake and processing to cyto-active fragments which can directly affect the transcription in the nucleus of cells, we have examined the binding, uptake and the cellular compartmentalization of HS-2 and HS-6 in both normal and transformed cells. Our data suggest that the antiproliferative effect of HS-6 on non-transformed cells may be due to its strong binding, high uptake and specific cellular localization to the nuclei of these cells.

MATERIALS AND METHODS

Materials

The HS fractions were prepared from beef lung, as described earlier [Fransson et al., 1980a; Fransson et al., 1980b; Arroyo-Yanguas et al., 1997; Malmström and Westergren-Thorsson, 1998]. In this study HS-2 and HS-6 were used and the detailed chemical data for HS-2 and HS-6 have been presented earlier [Fransson et al., 1979; Fransson et al., 1980b; Arroyo-Yanguas et al., 1997; Malmström and Westergren-Thorsson, 1998]. The HS-2 preparation employed contained approximately one-third IdoA, most of which was non-sulfated. In contrast, the HS-6 preparation contained approximately two-thirds IdoA, most of which was 2-O-sulfated. Human lung fibroblasts (HFL-1) and human lung carcinoma cells (A549) were purchased from the American Type Culture Collection. Eagle's minimal essential medium (EMEM) and newborn calf serum were obtained from Nord Vacc, Stockholm, Sweden. Chamber slides (four wells per slide, 3.75 cm^2 culture space per well) were purchased from Lab-Tek, Nunc International, Naperville, USA. Rhodamine 110 ($C_{20}H_{15}N_2O_3Cl$) was purchased from Molecular Probes, Amsterdam, The Netherlands.

Preparation of Iodine- or Rhodamine-Labeled Polysaccharide Derivatives

The ^{125}I-labeled HS-6 was prepared by coupling a p-hydroxyphenyl group to the peptide remnant at the reducing end, followed by iodination using chloramine T, as described [Arroyo-Yanguas et al., 1997].

In rhodamine labeling, HS chains were first released from their peptide by alkaline elimination [Cheng et al., 1992, 1994]. The aldehyde group of the reducing terminal xylose was coupled to rhodamine in the presence of sodium cyanoborohydride via reductive deamination [Cheng et al., 1994]. The tagged HS-preparations were purified by ion-exchange chromatography on DEAE-cellulose, which was washed with 6 M urea and 50 mM Tris buffer to remove free iodine or free fluorophore. The polysaccharide derivatives were eluted with 4M guanidine hydrochloride/0.05 M sodium acetate, and

finally recovered by ethanol precipitation [Cheng et al., 1992].

The degree of derivatisation was assessed by measuring the absorbance at A_{266} nm for the p-hydroxyphenyl group and at A_{488} nm for the rhodamine adducts. Generally the glycan chains incorporated 1 mole of p-hydroxyphenol or rhodamine per mole of GAG.

The purity of the HS-derivatives was assessed by 2% agarose gel electrophoresis and visualisation was by UV-light or by autoradiography.

Cell Culture and Growth Assay

Human lung fibroblasts and human lung carcinoma cells were cultured at 37°C in MEM supplemented with 10% newborn calf serum and 1% glutamine. For the cell growth assay, cells were seeded in 96-well microplates (Costar, Stockholm, Sweden) at a density of 3000 cells/well (A549) or 5000 cells/well (HFL-1), and allowed to plate for 5 h in MEM with 10% calf serum, followed by incubation in serum-free medium for 24 h. Growth was then initiated in Ham's F-12 medium containing insulin (10 μg/ml), transferrin (25 μg/ml) and epidermal growth factor (EGF) (20 ng/ml) as mitogen. The cultures were incubated for 96 h at 37°C with or without HS-6 solubilised in the medium with serum. Cell number was determined by the crystal violet method [Gillies et al., 1986]. For confocal microscopy cells were seeded in four-well chamber slides (3000 cells/well) and allowed to adhere for 4–6 h. Then the medium was changed to medium supplemented with HS-derivatives and cultures were incubated for various periods of time. Medium was then collected and the cells were washed twice with PBS. Finally, cells were fixed with methanol at room temperature for 5 min.

Cytotoxicity Assay

Cells were seeded in 96-well microplates and grown in Ham's F12 medium containing insulin (10 μg/ml) transferrin (25 μg/ml) and EGF (20 μg/ml) for various time periods in the presence of HS-6. After incubation, one set of microplates were centrifuged at $300 \times g$ for 10 min. For analysis of released lactate dehydrogenase (LDH), aliquots of the supernatant were transferred to clear flat-bottomed 96-well microplates. For analysis of total LDH, another set of microplates were sonicated using a Branson Sonifier Disruptor B15 and aliquots of the sonicates were transferred to the clear-bottomed plates. Estimations of LDH were performed using a LDH Cytotoxicity Detection Kit (Boehringer Mannheim, Germany). After addition of reagent, samples were incubated for 20 min and absorbance at 492 nm was measured using a Multiscan photometer.

Binding and Internalisation Studies

For binding and internalisation studies, cells were seeded in 24-well microplates. Cells were grown to confluence and were incubated with ^{125}I-labelled HS-2 (100 μg/ml) and HS-6 (100 μg/ml) for various lengths of time at 37°C. The medium was then removed and the cell monolayer was rinsed twice with fresh medium. Then the cells were incubated with 0.05% trypsin in PBS for 15–20 min at 37°C, and the resulting cell suspension was centrifuged (2,000 rpm for 3 min). HS-2 and HS-6 released by trypsin were considered to be bound to the cell surface. ^{125}I-labelled HS-2 and HS-6 remaining in the cell pellet after trypsin treatment were solubilized in 2% Triton-X100, re-centrifuged and the ^{125}I-labelled HS-2 and HS-6 recovered in this supernatant were considered to represent the HS taken up by the cells.

Scatchard plots were performed from cultures incubated with HS-2 or HS-6 at concentrations of 0.1–100 μg/ml for 4 h at 4°C. Free and bound material was measured as described above.

Confocal Microscopy

The confocal microscope used was a Nicon Eclipse E800, MRC-1024 (Bio-Rad). Excitation was obtained with an argon ion laser, supplying 0.3 mW continuous light to the specimen. For visualization of rhodamine-conjugated HS, the excitation wavelength of the confocal microscope was set at 488 nm and the emitted light was filtered with an appropriate long-pass filter (cut-off frequency 540 nm). Control cells were included in all experiments for correction of auto-fluorescence. Images were digitized and transferred to Adobe PhotoShop for merging, annotation and printing.

Characterization of Internalised HS

Internalised HS was collected according to the method described previously [Arroyo-Yanguas et al., 1997]. The HS from this pool (as described above) was purified by ion-exchange chromatography and examined by gradient polyacrylamide gel electrophoresis and visualized by UV

light. All steps of purification were monitored by fluorometery at Ex 488 nm and Em 520 nm. The image was obtained using a CCD camera and annotated in Adobe PhotoShop.

Statistical Methods

Mean ± SEM value was calculated. *t*-tests were used to evaluate the differences of the means between groups. *P*-values < 0.05 were considered significant.

RESULTS

Growth Effects and Cytotoxicity Assay

In a defined medium without serum the IdoA- and sulfate rich HS (HS-6) at a dose of 100 μg/ml inhibited growth by 30% ($P < 0.001$) of HFL-1 cells after 96 h incubation, while there was no significant effect on growth (3–12%) on A549 cells (Fig. 1). In contrast, the IdoA- and sulfate poor HS (HS-2) had no effects on the growth of either cell type. The growth inhibitory effect of HS-6 on HFL-1 cells was not due to cytotoxic effects measured as release of LDH (see inset). A similar inhibition of growth of HFL-1 cells with HS-6 has also been noted independently of serum or added growth factors in the medium [Westergren-Thorsson et al., 1993].

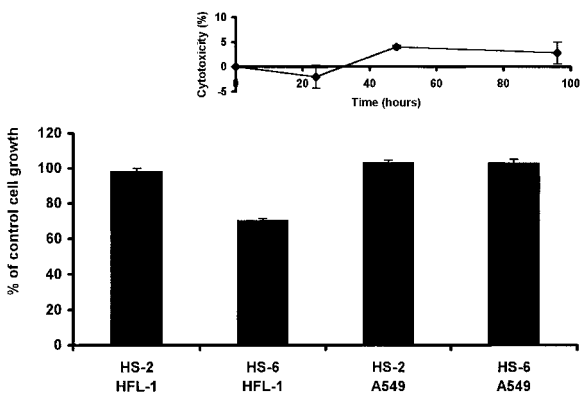

Fig. 1. Effect of exogenous HS on growth of human lung fibroblasts (HFL-1) and human lung carcinoma cells (A549). Growing cells were incubated with 100 μg/ml of HS-6 (high-sulfated and IdoA-rich) or HS-2 (low-sulfated and IdoA-poor) at 37°C for 96 h. In each experiment, a set of controls were performed. Cell number was measured by crystal violet and values are expressed as per cent of control. A cytotoxicity assay was carried out on the release of LDH. HFL-1 cells were incubated in triplicates with 100 μg/ml HS-6 for the indicated time-periods. The amounts of LDH were measured in the medium and in the total cell culture after sonication. The values were expressed as the percentage of LDH released into the medium in the presence of HS-6 (see inset). Values are shown as x ± SEM: n = 6; x = mean value.

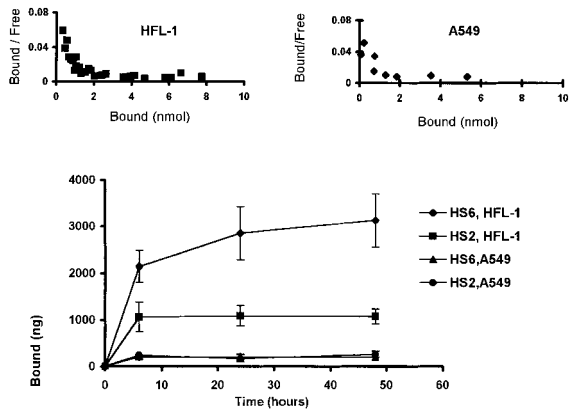

Fig. 2. Binding of HS-6 and HS-2 to HFL-1 and A549 cells. Cells were incubated with 100 μg/ml ^{125}I-labeled HS-2 (low-sulfated and IdoA-poor) and HS-6 (high-sulfated and IdoA-rich) at 37°C for various times and the amount of bound material was measured (for details see Methods). Values are shown as x ± SEM; n = 4. The inserts show Scatchard plots of binding of HS-6 to HFL-1 cells (left) and A549 cells (right). Cultures were incubated with HS-6 in concentrations between 0.05–100 μg/ml at 4°C. One representative experiment out of six is shown.

Binding Sites

The time course of binding and internalization of ^{125}I-labelled HS-6 or HS-2 to HFL-1 and A549 cells at 37°C was compared and is shown in Fig. 2. GAGs that remained free in the medium, bound or internalized was determined (for details see Material and Methods). The saturation level of binding was usually reached between 6 and 24 h (Fig. 2). At a concentration of 100 μg/ml A549 cells bound considerably less (0.25%) of both HS-6 and HS-2 (Fig. 2) than HFL-1 cells, which almost bound 3% of the added HS-6 and approximately 1% of the added HS-2 (Fig. 2) [Arroyo-Yanguas et al., 1997]. To further study the number of binding sites, HFL-1 and A549 cells were incubated for 4 h at 4°C with different concentrations of HS-2 and HS-6. The binding data are presented as Scatchard plots and only the binding of HS-6 to the two cell types is shown (Fig. 2 insets). The plots indicate the existence of two binding sites for both HS-6 (Fig. 2, insets) and HS-2 (data not shown) to HFL-1 cells. The dissociation constant (K_d) for HFL-1 cells for the high affinity site and the low affinity site was similar for both types of GAGs, which also have been indicated earlier in the study by Arroyo-Yanguas et al. [1997]. The K_d values for the high affinity site

were 6 and 6.9×10^{-8} M and for the low affinity site 4.7 and 2.9×10^{-6} M for HS-6 and HS-2, respectively. Also A549 cells had two binding sites for HS-6 (Fig. 2 inset) but, however, only one binding site for HS-2 (data not shown). In A549 cells the dissociation constant for HS-6 were somewhat lower than for the HFL-1 cells, with a K_d of 3.5×10^{-6} M and 4×10^{-5} M for the high and low affinity sites, respectively. The K_d for binding of HS-2 to A549 cells was 6×10^{-7} M (data not shown).

Uptake Assays

Radiolabeled HS-2 and HS-6 (100 μg/well) was added to cells at 37°C, and after various time periods the cell layer was trypsinized. Released cells were collected by centrifugation and lysed with detergent. A steady state level of internalization was usually reached within 24 h (Fig. 3). At 48 h, HS-6 was internalized to a 3-fold greater extent than HS-2 in HFL-1 cells (Fig. 3) [Arroyo-Yanguas et al., 1997].

In A549 cells, uptake of HS-6 and HS-2 was much lower than uptake in HFL-1 cells. However, the proportions of bound material (see Fig. 2) taken up by HFL-1 and A549 cells were similar (approximately 10%).

Cellular Localization

Uptake of rhodamine-tagged HS by HFL-1 or A549 cells was further studied by confocal microscopy. Also by this method, HS-6 was internalized to a much greater extent than HS-2 in HFL-1 cells. At time points up to 24 h, HS-6 was found and accumulated with time in the cytoplasm (Fig. 4G). At later time points, HS-6 was found with a peri-nuclear localization, and after 48 h incubation it started to appear in the nucleus. At 72 h, HS-6 was mostly localized to the nucleus, reaching a maximum uptake in this compartment at that time point (Fig. 4H). With larger magnification it could be seen that HS-6 was evenly distributed in the nucleus (Fig. 4J) and after 96 h of incubation, the HS-6 signal in the nucleus started to fade (Fig. 4I). In a control experiment with a ten-fold excess of unlabeled HS-6, the nuclear localization of rhodamine-tagged HS-6 disappeared and only some signal in the cytoplasm could be obtained (Fig. 4K). No signal at all was seen in cells from cultures incubated with a twenty-fold excess of unlabelled HS-6 (Fig. 4L).

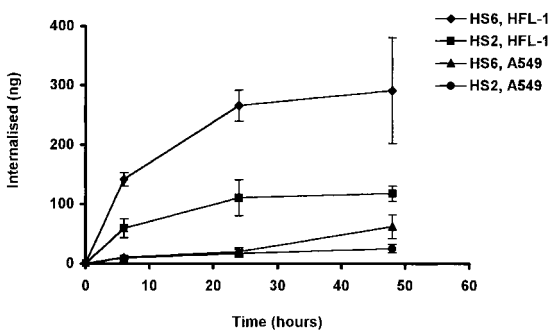

Fig. 3. Internalization of HS-2 and HS-6 by HFL-1 and A549 cells. Cells were incubated with 100 μg/ml of ^{125}I-labelled HS-2 (low-sulfated and IdoA-poor) and HS-6 (high-sulfated and IdoA-rich) at 37°C for various time-periods and the amount of internalized HS was analyzed (for details see Methods). Values are shown as x ± SEM; n = 4.

In contrast to HS-6, there was a small and slow uptake of HS-2 by HFL-1 cells (Fig. 4B). After 72 h incubation, the uptake of HS-2 reached a maximum and the localization HS-2 was restricted to some peri-nuclear areas, probably in endosomes or lysosomes (Fig. 4C and E). The localization of HS-2 was the same after 96 h incubation (Fig. 4D).

In A549 cells, HS-6 was internalized to some extent in a time-dependent manner (Fig. 5F–I). After 48 h of incubation, HS-6 was detected in the nucleus (Fig. 5F). Uptake of HS-6 was time-dependent and was restricted to areas near the nuclear membrane (Fig. 5G). After 96 h, most of the nuclei were stained in this way (Fig. 5H). At larger magnification, it is evident that staining was mainly confined to the periphery of the nucleus and formed specific ring structures (Fig. 5I). The uptake and localization of HS-2 in A549 cells were negligible (Fig. 5B–D). Figure 4A and F, Figure 5A and E are control cultures where no rhodamine-tagged HS was added, showing that there was no auto-fluorescence.

Characterization of the Internalized HS-6 in HFL-1 Cells

After 72 h, incubation with rhodamine-tagged HS-6 in HFL-1 cells, the internalized pool was recovered to exclude the possibility that the staining in the nucleus emanated from free rhodamine. At this time point the recovered and internalized material mainly originated from the nucleus (see Fig. 4H and J). Figure 6 shows that the internalized HS-6 was somewhat processed (lane 2) compared to rhodamine-tagged HS-6 alone (lane 1). It further shows that no free rhodamine could be detected

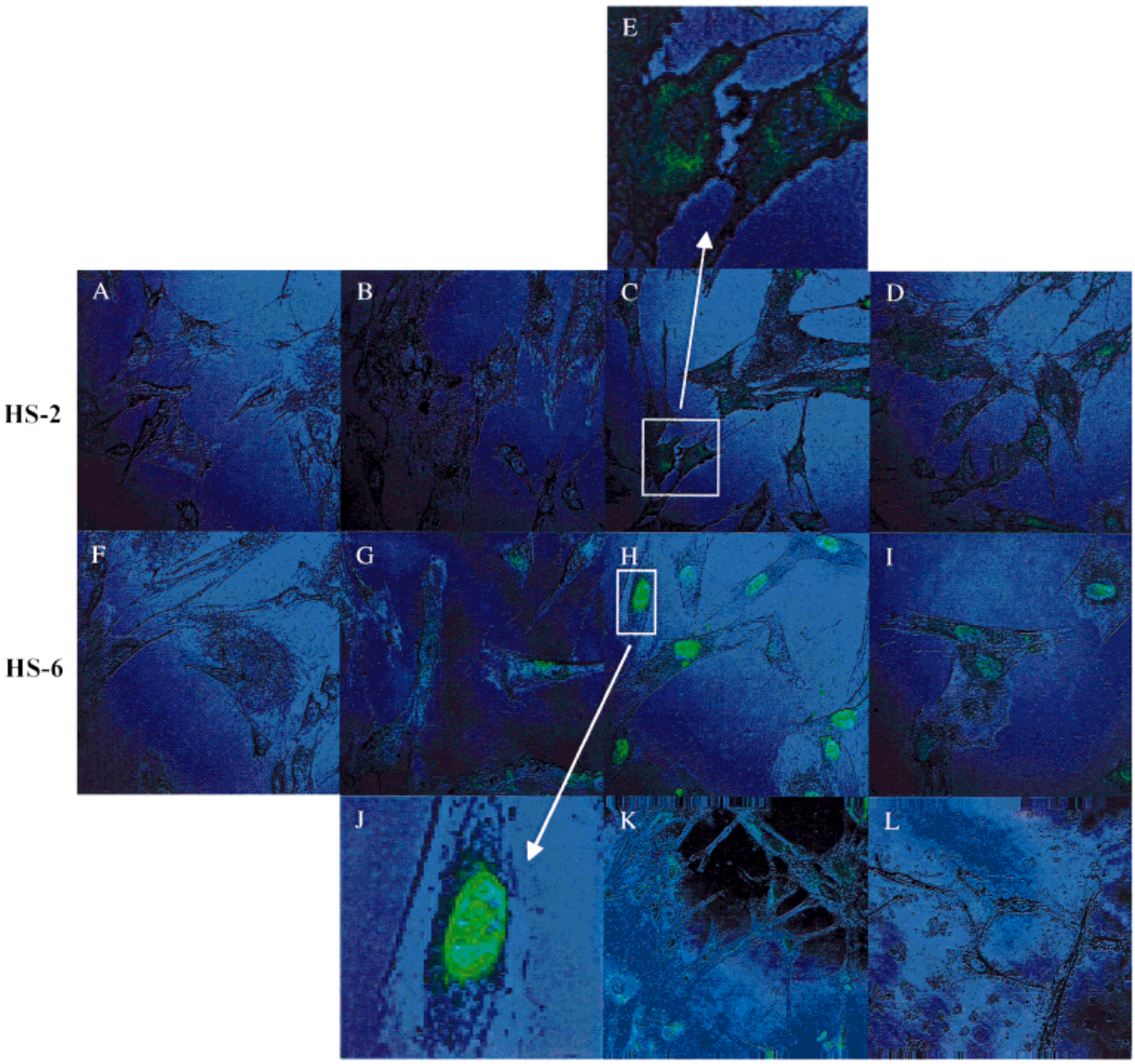

Fig. 4. Localization by confocal microscopy of rhodamine-labeled HS-2 (low-sulfated and IdoA-poor) and HS-6 (high-sulfated and IdoA-rich) in HFL-1 cells. Cells were incubated with 50 μg/ml of rhodamine-labeled HS-2 or HS-6 at 37°C for 0 h (**A**, **F**), 24 h (**B**, **G**), 72 h (**C**, **H**) and 96 h (**D**, **I**). Blow-ups are shown in (**E**) and (**J**) from cultures incubated with HS-2 and HS-6, respectively. Cells were also incubated with 50 μg/ml rhodamine-labeled HS-6 together with 500 μg/ml or 1 mg/ml unlabelled HS-6, shown in (**K**) respectively (**L**). One out of four experiments is shown.

in the internalized HS pool (lane 2 compared to lane 3(free rhodamine)).

DISCUSSION

Highly sulfated and IdoA-rich HS (HS-6) inhibited growth of human lung fibroblasts (HFL-1) but not of human lung carcinoma cells (A549). A sulfate- and IdoA-poor HS (HS-2) had no effect on the growth of either type of cells. To further explore the possible mechanism behind the antiproliferative effect, binding, uptake, and localization were examined by use of ^{125}I and fluorescence labeled HS.

Using confocal microscopy, visualization of the nuclear localization of the antiproliferative HS-6 in HFL-1 cells was possible, whereas the non-antiproliferative HS-2 was localized in the perinuclear compartment in this cell type. Furthermore, in HFL-1 cells, the antiproliferative ^{125}I- labeled HS-6 bound 3-fold more to the cell surface than the non-antiproliferative HS-2, shown in this study and also by Arroyo-Yanguas et al. [1997]. The extent of uptake of

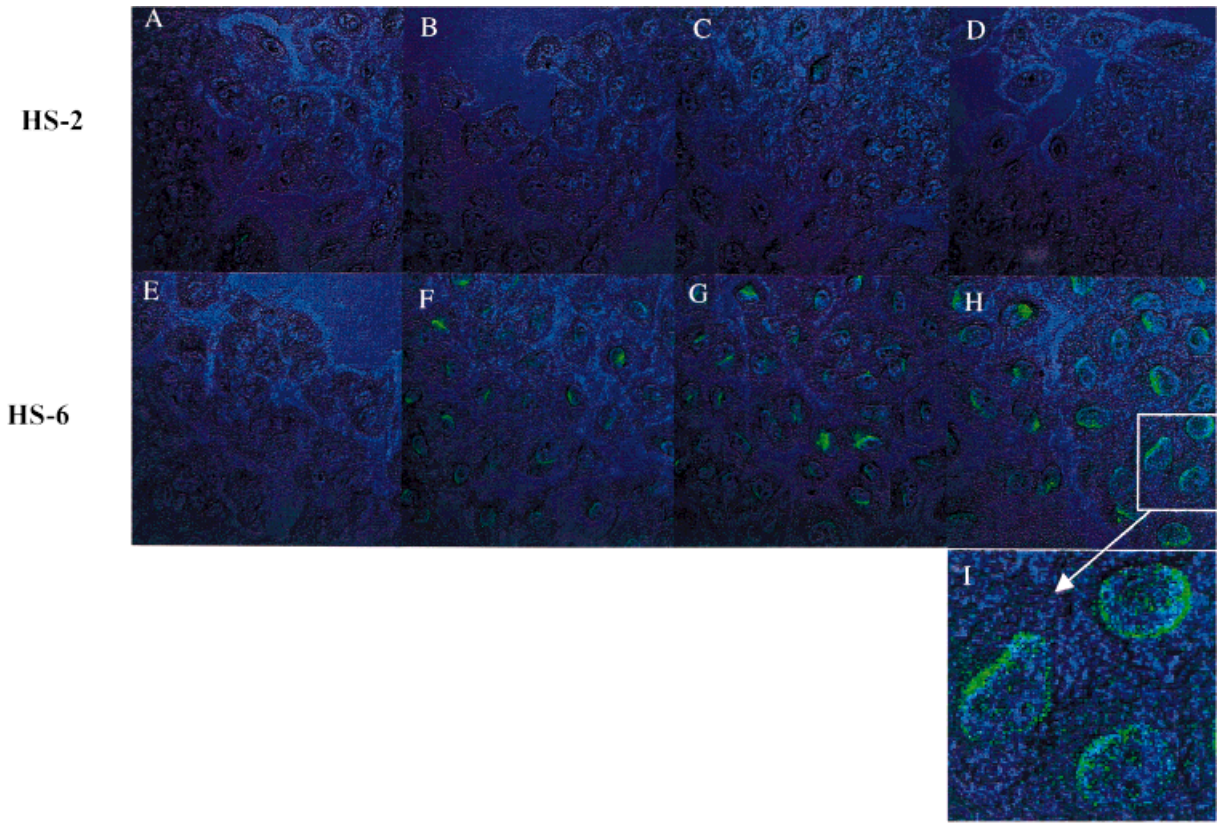

Fig. 5. Localization by confocal microscopy of rhodamine-labeled HS-2 (low-sulfated and IdoA-poor) and HS-6 (high-sulfated and IdoA-rich) in A549 cells. Cells were incubated with 50 μg/ml rhodamine-labeled HS-2 (upper panel) or HS-6 (lower panel) at 37°C for 0 h (**A**, **E**), 48 h (**B**, **F**), 72 h (**C**, **G**) and 96 h (**D**, **H**). Blow-up of culture incubated with HS-6 is shown in (**I**). One experiment out of three is shown.

HS-6 was twice as high as that of HS-2, suggesting that a high content of sulfate and IdoA are necessary for binding and internalization, as well as for nuclear localization. Nuclear localization and growth inhibition both appeared after 48 h of incubation, suggesting that the antiproliferative effect is exerted in the nucleus of HFL-1 cells. HS-6 and/or its products may interfere with nuclear events, for instance by interference with transcription interaction factors such as *c-fos, c-jun, and c-myc* [Ottlinger et al., 1993; Herbert et al., 1996; Miralem et al., 1996; Ueda et al., 1996] or repression of transcription of *cis*-activating elements such as of AP-1 [Busch et al., 1992], SP-1, ETS-1 and NFκB [Dudás et al., 2000]. Other ways to effect nuclear events is the findings that heparin decreases the activity of signal transduction pathways, such as the pathway for MAPkinase [Ottlinger et al., 1993].

There are several possibilities for HS to achieve nuclear localization. Arroyo-Yanguas et al. [1997] have reported two binding sites for HS-6, where the low affinity receptor with a K_d in the order of 10^{-6} most likely is an endocytosis receptor, important for the internalization process. HS proteoglycans have been proposed to be internalized through endcytosis receptors in caveolae [Gleizes et al., 1995], where also several growth factor receptors have been found including the receptors of PDGF [Liu et al., 1997]. The exact structure of the endocytosis receptor is, however, unknown. Possible other candidates are FGF-receptors [Takagi et al., 1994], PDGF-receptors [Malmström and Westergren-Thorsson, 1998] and the decorin receptor [Hausser and Kresse, 1991] and co-internalization with polyamines is also a possibility [Belting et al., 1999]. Endocytosis is likely followed by processing, which is indicated in Figure 6, showing that HS in the nucleus are processed and somewhat shorter in HFL-1 cells. This is in agreement with the study of Fedarko and Conrad [1986], where they suggested that internalized HS might be processed to fragments specifically containing 2–*O*-sulfated

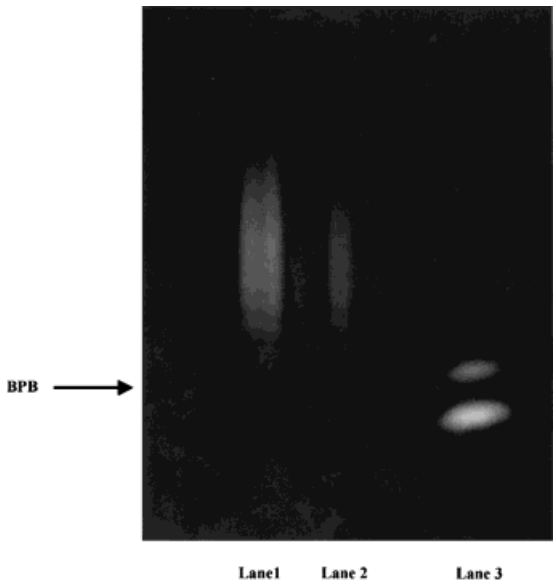

Fig. 6. Characterization of size of internalized rhodamine-labeled HS-6 in HFL-1 cells by polyacrylamide gel electrophoresis. HS-6 (high-sulfated and IdoA-rich) from the internalized pool was recovered and purified on DEAE-cellulose (for details see Methods). It was subjected to polyacrylamide gel electrophoresis and visualized by UV-light. **Lane 1**: rhodamine-labeled HS-6 alone; **lane 2**, internalized rhodamine-labeled HS-6; **lane 3**, free rhodamine. The molecular weight of BPB, bromphenol blue, is marked to the left, indicating the migration position of an oligosaccharide with the general carbohydrate backbone structure $(HexA\text{-}GalNAc)_4$-GlcA-Gal-Gal-Xyl-R.

GlcA-residues. Accumulation of these oligosaccharides in the nuclei correlated with arrest of cell growth. However, these data were based on cell sub-fractionation and did not provide direct identification of the cellular location of HS. Several other reports [Hiscock et al., 1994; Barzu et al., 1996] claim that HS is never to be found in the nucleus, and was most often located around the nucleus. They also demonstrated that it was very difficult to obtain a pure nuclear preparation, implying that results based on cellular fractionation might be due to preparation artifacts. Another possibility to achieve nuclear localization is the presence of a nuclear localization code in the core protein, demonstrated in the HS proteoglycan glypican, which results in transport to the nuclei of neurons and glioma cells [Liang et al., 1997].

An observation of potential interest is the fact that HS with a specific structure is required for inhibition of cell growth, and furthermore, the finding that the human transformed cell line, A549 could escape this inhibition. Several mechanisms for this escape have been used by these cells, such as low binding, low uptake, and in addition, different localization. In A549 cells, HS-6 was localized to the periphery of the nuclei, where heterochromatin should be abundant. This is in contrast to HFL-1 cells, where HS-6 was uniformly distributed, *i.e.,* also over the euchromatin areas. This may explain why cancer cells usually can escape control, and display unrestrained growth. It is not possible to exclude, however, that HS-6 could have antiproliferative effect in A549 cells, provided that the intracellular concentration of HS-6 could be similar to that in HFL-1 cells. This is however not the case, as HS6 bind less with lower affinity to A549 cells, resulting in lower uptake.

Several other possibilities whereby HS can control cell growth have been proposed, for example by affecting cell adhesion [Liu et al., 1998; Woods and Couchman, 1998], migration [Davies et al., 1999] and regulation of cell surface receptors [Keifer et al., 1990; Yayon et al., 1991; Gallagher and Turnbull, 1992; Malmström and Westergren-Thorsson, 1998]. To further understand the mechanism behind the antiproliferative effect of HS-6, the above effects on cell growth must further be evaluated against nuclear localization and the ensuing effect on gene expression.

ACKNOWLEDGMENTS

The expert technical assistance of Urszula Endresén, Lena Åberg and Susanne Persson is gratefully acknowledged. We also would like to acknowledge Prof. Catharina Svanborg, Department of Micobiology, Immunology and Glycobiology, Lund, Sweden, for kindly letting us use the confocal microscope.

REFERENCES

Arroyo-Yanguas Y, Cheng F, Isaksson A, Fransson L-Å, Malmström A, Westergren-Thorsson G. 1997. Binding, internalization, and degradation of antiproliferative heparan sulphate by human embryonic lung fibroblasts. J Cell Biochem 64:595–604.

Barzu T, Pascal M, Maman M, Roque C, Lafont F, Rousselet A. 1996. Entry and distribution of fluorescent antiproliferative heparin derivatives into rat vascular smooth muscle cells. Comparison between heparin-sensitive and heparin-resistant cultures. J Cell Physiol 167:8–21.

Belting M, Persson S, Fransson L-Å. 1999. Proteoglycan involvement in polyamine uptake. Biochem J 338:317–323.

Bernfield M, Götte M, Park PW, Reizes O, Fitzgerald ML, Linececum J, Zako M. 1999. Functions of cell surface heparan sulfate proteoglycans. Annu Rev Biochem 68:729–777.

Busch SJ, Martin GA, Barnhart RL, Mano M, Cardin AD, Jackson RL. 1992. Trans-repressor activity of nuclear glycosaminoglycans on Fos and Jun/Ap1 oncoprotien-mediated transcription. J Cell Biol 116:31–42.

Castellot JJ, Wong K, Herman B, Hoover RL, Albertini DF, Wright TC, Caleb BL, Karnovsky MJ. 1985. Binding and internalization of heparin by vascular smooth muscle cells. J Cell Physiol 124:13–20.

Cheng F, Yoshida K, Heinegård D, Fransson L-Å. 1992. A new method for sequence analysis of glycosaminoglycans from heavily substituted proteoglycans reveals non-random positioning of 4- and 6-O-sulphated N-acetylgalactosamine in aggrecan-derived chondroitin sulphate. Glycobiology 2:553–561.

Cheng F, Heinegård D, Malmström A, Schmidtchen A, Yoshida K, Fransson L-Å. 1994. Patterns of uronosyl epimerization and 4-/6-O-sulphation in chondroitin/dermatan sulphate from decorin and biglycan of various bovine tissues. Glycobiology 4:685–696.

Cifonelli JA, King JA. 1977. Structural characteristics of heparan sulfates with varying sulfate contents. Biochemistry 16:2137–2141.

Davies Y, Lewis D, Fullwood NJ, Nieduszynski IA, Marcyniuk B, Albon J, Tullo A. 1999. Proteoglycans on normal and migrating human corneal endothelium. Exp Eye Res 68:303–311.

Dudás J, Ramadori G, Knittel T, Neubauer K, Raddatz D, Egedy K, Kovalszky I. 2000. Effect of heparin and liver heparan sulphate on interaction of HepG2-derived transcription factors and their *cis*-acting elements: Altered potential of hepatocellular carcinoma heparan sulphate. Biochem J 350:245–251.

Elenius K, Salmivirta M, Inki P, Mali M, Jalkanen M. 1990. Binding of human syndecan to extracellular matrix proteins. J Biol Chem 265:17837–17843.

Fedarko NS, Conrad HE. 1986. A unique heparan sulphate in the nuclei of hepatocytes: structural changes with the growth state of the cells. J Cell Biol 102:587–599.

Fransson L-Å, Nieduszynski IA, Phelps CF, Sheehan JK. 1979. Interactions between dermatan sulfate chains. Light-scattering and viscometry studies of self-association. Biochim Biophys Acta 586:179–188.

Fransson L-Å, Nieduszynski LA, Sheehan JK. 1980a. Interaction between heparan sulphate chains. A gel chromatographic, light-scattering and structural study of aggregating and non-aggregating chains. Biochim Biophys Acta 630:287–300.

Fransson L-Å, Sjöberg I, Havsmark B. 1980b. Structural studies on heparan sulphates. Characterization of oligosaccharides; obtained by periodate oxidation and alkaline elimination. Eur J Biochem 106:59–69.

Gallagher JT, Turnbull JE. 1992. Heparan sulphate in the binding and activation of basic fibroblast growth factor. Glycobiology 2:523–528.

Gallagher JT, Lyon M, Steward WP. 1986. Structure and function of heparan sulphate proteoglycans. Biochem J 236:313–325.

Gillies RJ, Didier N, Denton M. 1986. Determination of cell number in monolayer cultures. Anal Biochem 159:109–113.

Gleizes PE, Noaillac-Depeyre J, Amalric F, Gas N. 1995. Basic fibroblast growth factor (FGF-2) internalization through the heparan sulafte proteoglycans-mediated pathway: an ultrastructural approach. Eur J Cell Biol 66:47–59.

Hausser H, Kresse H. 1991. Binding of heparin and of the small proteoglycan decorin to the same endocytosis receptor proteins leads to different metabolic consequences. J Cell Biol 114:45–52.

Herbert JM, Clowes M, Lea HJ, Pascal M, Clowes AW. 1996. Protein kinase C alpha expression is required for heparin inhibition of rat smooth muscle cell proliferation in vitro and in vivo. J Biol Chem 271:25928–25935.

Hiscock DR, Yanagishita M, Hascall VC. 1994. Nuclear localization of glycosaminoglycans in rat ovarian granulosa cells. J Biol Chem 269:4539–4546.

Iozzo RV. 1998. Matrix proteoglycans: From molecular design to cellular function. Ann Rev Biochem 57:609–623.

Keifer MC, Stephans JC, Crawford K, Okino K, Barr P.J. 1990. Ligand affinity cloning and structure of a cell surface heparan sulfate proteoglycan that binds basic fibroblast growth factor. Proc Natl Acad Sci USA 87:6985–6989.

Kjellén L, Lindahl U. 1991. Proteoglycans: Structure and interactions. Annu Rev Biochem 60:443–475.

Liang Y, Haring M, Roughley PJ, Margolis RK, Margolis RU. 1997. Glypican and biglycan in the nuclei of neurons and glioma cells: presence of functional nuclear localization signals and dynamic changes in glypican during the cell cycle. J Cell Biol 139(4):851–864.

Linker A, Hovingh P. 1975. Structural studies of heparan sulfates. Biochim Biophys Acta 385:324–333.

Liu P, Ying Y, Anderson RG. 1997. Heparan sulfate proteoglycans as adhesive and antinvasive molecules. Syndecans and glypican have distinct functions. Proc Natl Acad Sci USA 94(25):13666–13670.

Liu W, Litwack ED, Stanley MJ, Langford JK, Lander AD, Sanderson RD. 1998. Heparan sulfate proteoglycans as adhesive and anti-invasive molecules. Syndecans and glypican have distinct functions. J Biol Chem 273: 22825–22832.

Malmström J, Westergren-Thorsson G. 1998. Heparan sulfate upregulates platelet-derived growth factor receptors on human lung fibroblasts. Glycobiology 8:1149–1155.

Miralem T, Wang A, Whiteside CI, Templeton DM. 1996. Heparin inhibits mitogen-activated protien kinase-dependent and — independent *c-fos* induction of mesangial cells. J Biol Chem 271:17100–17106.

Ottlinger ME, Pukac LA, Karnovsky MJ. 1993. Heparin inhibits mitogen activated protein kinase activation in intact rat vascular smooth muscle cells. J Biol Chem 268:19173–19176.

Pukac LA, Castellot JJJ, Wright TCJ, Caleb BL, Karnovsky MJ. 1990. Heparin inhibits *c-fos* and *c-myc* mRNA expression in vascular smooth muscle cells. Cell Regul 1:435–443.

Redini F, Moczar E, Antoine E, Poupon MF. 1989. Binding and internalization of exogenous glycosaminoglycans in weakly and highly meastatic rhabdomyosarcoma cells. Biochim Biophys Acta 991:359–366.

Salmivirta M, Lidholt K, Lindahl U. 1996. Heparan sulfate: a piece of information. FASEB-J 10:1270–1279.

Taipala J, Keski-Oja J. 1997. Growth factors in the extracellular matrix. FASEB-J 11:515–519.

Takagi Y, Shrivastav S, Miki T, Sakaguchi K. 1994. Molecular cloning and expression of the acidic fibroblast growth factor receptors in a rat parathyroid cell line (PT-r). Parathyroid cell- specific calcium-dependent change of ligand accessibility and covalent attachment of heparan sulfate glycosaminoglycan to the receptors. J. Biol Chem 269:23743–23749.

Ueda Y, Hirai S, Osada S, Suzuki A, Mizuno K, Ohno S. 1996. Protein kinase C activates the MEK-ERK pathway in a manner independent of Ras and dependent on Raf. J Biol Chem 271:23512–23519.

Vannucchi S, Pasquali F, Porciatti F, Chiarugi V, Magnelli L, Bianchini P. 1988. Binding, internalization and degradation of heparin and heparin fragments by cultured endothelial cells. Thromb Res 49:373–383.

Westergren-Thorsson G, Önnervik P.O, Fransson L-Å, Malmström A. 1991. Proliferation of cultured fibroblasts is inhibited by L-iduronate-containing glycosaminoglycans. J Cell Physiol 147:523–530.

Westergren-Thorsson G, Persson S, Isaksson A, Önnervik P-O, Malmstöm A, Fransson L-Å. 1993. L-Iduronate-rich glycosaminoglycans inhibit growth of normal fibroblasts independently of serum or added growth factors. Exp. Cell Res 206:93–99.

Woods A, Couchman JR. 1998. Syndecans: synergistic activators of cell adhesion. Trends Cell Biol 8:189–192.

Wright TC, Castellot JJJ, Diamond JR, Karnovsky MJ. 1989a. D.A. Lane Heparin, Lindahl U, editors. Regulation of cellular proliferation of heparin and heparan sulphate. London: Edward Arnold. 295–316.

Wright TC, Pukac LA, Castellot JJJ, Karnovsky MJ, Levine RA, Kim-Park HY, Campisi J. 1989b. Heparin suppresses the induction of *c-fos* and *c-myc* mRNA in murine fibroblasts by selective inhibition of a protein kinase C-dependent pathway. Proc Natl Acad Sci USA 86:3199–3203.

Yayon A, Klagsbrun M, Esko JD, Leder P, Ornitz DM. 1991. Cell surface, heparin-like molecules are required for binding of basic fibroblast growth factor to its high affinity receptor. Cell 64:841–848.